Tumor Imaging

DOI: 10.1002/ange.201101005

High-Contrast Fluorescence Imaging of Tumors In Vivo Using Nanoparticles of Amphiphilic Brush-Like Copolymers Produced by ROMP**

*Koji Miki, Akinori Kimura, Kazuaki Oride, Yoshiaki Kuramochi, Hideki Matsuoka, Hiroshi Harada, Masahiro Hiraoka, and Kouichi Ohe**

Optical imaging techniques used to detect malignant tumors by endoscopy or at surgery require near-infrared fluorescence (NIRF) probes containing dyes with high signal-to-noise (S/N) ratios.[1] Along with a high S/N ratio in the near-infrared spectral region, these probes must accumulate specifically in the targeted tumor tissues. Spherical amphiphilic assemblies with diameters of 50–200 nm, such as liposomes, liposome-like assemblies,[2] and micelles or vesicles of polymer conjugates,[3] have been investigated with the expectation that they accumulate in solid tumors because of their enhanced permeability and retention (EPR) effect.[4]

Optical tumor imaging faces two problems. The first problem is the stability of the self-assembled amphiphilic copolymers. The disassembly of amphiphiles under diluted conditions, especially in blood vessels, reduces both their S/N ratio and specificity as probes for tumors. The second problem concerns the fluorescence intensities. Hydrophobic dyes attached to copolymers are prone to aggregate in aqueous solution, and self-quenching therefore reduces the quantum yields.[5] To address the first problem, we focused our attention on the cross-linked assemblies of copolymers with hydrophobic and hydrophilic polymeric side chains (Figure 1). Because the polymer backbone bearing hydrophobic and hydrophilic polymeric side chains forms a part of a permeable interface between a hydrophobic core and hydrophilic shell,[6] the self-assemblies are expected to be highly stable. Additionally, partial cross-linking of the interface preserves the mobility of hydrophobic dyes dispersed in the hydrophobic core. Therefore, we assumed that the dispersed hydrophobic dyes conjugated with long side chains inherently emit fluorescence even in aqueous media (Figure 2).

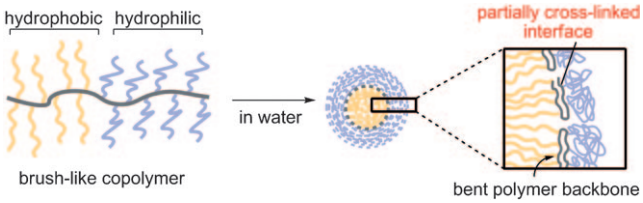

Figure 1. Amphiphilic polymer brushes which form spherical self-assemblies in aqueous media.

Ring-opening metathesis polymerization (ROMP) of strained bicyclic compounds was used to produce readily multiblock copolymers and random copolymers in high yields with a low polydispersity index.[7] The synthetic method, living ROMP, and its compatibility with highly functional groups are found to be most important for the preparation of highly functionalized amphiphilic copolymers that form spherical nanoparticles for tumor therapy and imaging.[8,9] Although several amphiphilic brush-like copolymers with polymeric side chains obtained by ROMP have been reported to form self-assemblies,[10] to the best of our knowledge, there is no

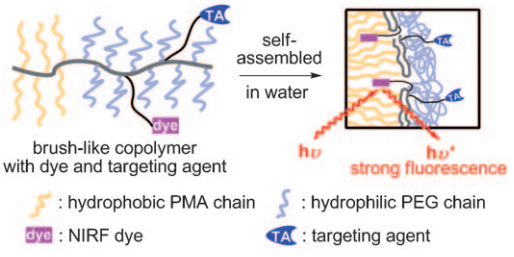

Figure 2. Self-assemblies consisting of PMA and PEG-grafted amphiphilic brush-like copolymers used as imaging probes.

[*] Dr. K. Miki, A. Kimura, K. Oride, Y. Kuramochi, Prof. K. Ohe
Department of Energy and Hydrocarbon Chemistry
Graduate School of Engineering, Kyoto University
Katsura, Nishikyo-ku, Kyoto 615-8510 (Japan)
Fax: (+81) 75-383-2499
E-mail: ohe@scl.kyoto-u.ac.jp
Homepage: http://www.ehcc.kyoto-u.ac.jp/eh31/home2/index.html
Prof. H. Matsuoka
Department of Polymer Chemistry, Graduate School of Engineering
Kyoto University, Katsura, Nishikyo-ku, Kyoto 615-8510 (Japan)
Dr. H. Harada
Group of Radiation and Tumor Biology, Career-Path Promotion Unit for Young Life Scientists, Kyoto University, Yoshida Konoe-cho, Sakyo-ku, Kyoto 606-8501 (Japan)
Prof. M. Hiraoka
Department of Radiation Oncology and Image-Applied Therapy
Graduate School of Medicine, Kyoto University
54 Shogoin Kawahara-cho, Sakyo-ku, Kyoto 606-8507 (Japan)

[**] This work was supported by the Research for Promoting Technological Seeds from the Japan Science and Technology Agency and the Program for Promotion of Fundamental Studies in Health Science of the National Institute of Biomedical Innovation (NIBIO, Japan). We acknowledge Prof. Takeshi Abe and Dr. Kohei Miyazaki at Kyoto University for TEM measurements and Akiyo Morinibu at Kyoto University for technical assistance with the in vivo imaging experiments. ROMP = ring-opening metathesis polymerization.

Supporting information for this article is available on the WWW under http://dx.doi.org/10.1002/anie.201101005.

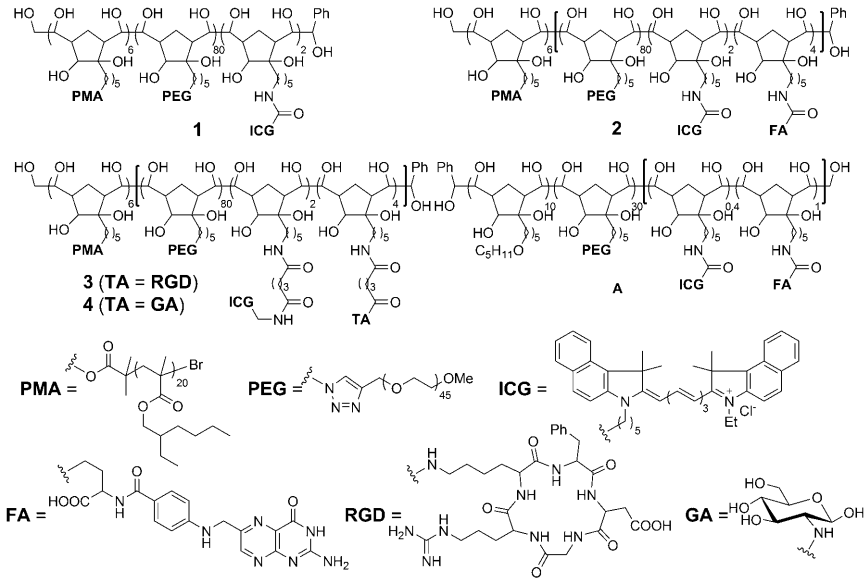

Figure 3. Amphiphilic copolymers **A** and **1**–**4**. All segments inside bold brackets were polymerized randomly; M_n(PMA) = 5400 and M_n(PEG) = 2000.

example for their application to tumor imaging in vivo. We report here high-contrast tumor imaging probes consisting of polymer backbones bearing poly(methacrylate) (PMA) and poly(ethylene glycol) (PEG) polymer brushes, which are obtained by ROMP.

The synthesis of copolymers **1**–**4** bearing hydrophobic and hydrophilic polymer brushes includes ROMP to introduce PMA moieties as hydrophobic segments, copper-catalyzed [2+3] cyclization[11] to graft PEG segments, and dihydroxylation[12] of double bonds in the main chain of the polymer (Figure 3). We prepared random copolymers of PEG, the NIRF indocyanine green (ICG) dye, and targeting-agent segments, followed by end-capping reactions of PMA macromonomers to obtain PMA-grafted copolymers.[13,14] The random copolymerization enhanced the fluorescence intensities of the amphiphilic copolymer assemblies because the self-quenching of the dye moieties was restricted (see Figure S4 in the Supporting Information). The folate-containing copolymer **A**, which forms self-assemblies without cross-linked interface, was also prepared as control sample.[9b] For its conjugation with cyclic RGD peptides (RGD) and glucosamine molecules (GA) as targeting agents, we synthesized a new ICG derivative[15] bearing an amino functional group, which readily reacts with carboxyl groups on the polymer side chains of random copolymers.

Table 1: Diameters, critical aggregation concentrations, and fluorescence intensities of the self-assembled copolymers **1**–**4** and **A**.

Polymer	D_{TEM} [nm][a]	D_{DLS} [nm][b]	cac [g L^{-1}][c]	Relative FL intensity[d]
1	170 ± 37	194	8.1×10^{-5}	1.00
2	164 ± 37	216	6.7×10^{-5}	0.83–0.88
3	163 ± 49	204	1.4×10^{-5}	3.68–3.76
4	151 ± 46	212	4.0×10^{-5}	3.56–3.67
A	158 ± 32	182	5.5×10^{-4}	–

[a] Distribution of the diameters of nanoparticles determined by TEM. [b] Hydrodynamic diameters of nanoparticles in aqueous solution measured by DLS. [c] Measured by SLS. [d] Fluorescence intensities of **2**–**4** relative to that of **1** in aqueous solution (10 mg mL^{-1}).

All copolymers **1**–**4** were dissolved in aqueous solution and formed nanometer-sized self-assemblies (Table 1). The molecular weights of copolymers **1**–**4** were about three times as large as that of copolymer **A**, whereas the diameters of the nanoparticles formed by copolymers **1**–**4** were slightly larger than that of **A** as observed by transmission electron microscopy (TEM) and dynamic light scattering (DLS).[16] This slight difference in the diameters might be caused by the high-density cohesion of the hydrophobic cores in the polymeric self-assemblies. Because the critical aggregation concentrations (cac) estimated by static light scattering (SLS) were 7–40 times lower than that of copolymer **A**, self-assemblies of copolymers **1**–**4** were extremely stable under diluted conditions in aqueous solution.[17] The stronger fluorescence of assemblies of copolymers **3** and **4** relative to that of **1** and **2** indicates that hydrophobic ICG dye moieties tethered by long side chains, which could enhance their mobility, prefer to disperse in the hydrophobic core of the assemblies and thereby display inherent fluorescence.

To examine the characteristics of the brush-like copolymers **1**–**4** as tumor-specific probes in vivo, we performed a series of optical imaging experiments (Figure 4). We intravenously injected polymer conjugates **1**–**4** into nude mice bearing a subcutaneous tumor xenograft[18] in their right hind leg and monitored their distribution using an optical in vivo imaging device.[19] The probes gradually accumulated in tumor tissues, and their fluorescence intensities exceeded the threshold level within six hours after injection. As shown in Figure 4a, the tumor site could be visualized through the EPR effect of copolymer **1**, despite the strong fluorescence from the liver.[20] The accumulation of copolymer **2** in the liver relative to that of copolymer **1** was slightly suppressed by the effect of folate-receptor targeting (Figure 4b). In contrast, optical in vivo imaging of copolymers **3** and **4** afforded high-contrast images of clearly visualized tumor sites (Figure 4c,d). We measured fluorescence intensities in two defined regions of interest (ROIs): at a tumor site (ROI 1) and in the liver and kidney (ROI 2, Figure 5a). The fluorescence intensities of copolymers **3** and **4** in the tumor sites were four to six times as strong as those of copolymers **1** and **2** (Figure 5b). The contrast ratios (defined as the ratio of fluorescence intensities of ROIs 1 and 2) show that copolymers **1** and **2** did not accumulate efficiently in the tumor tissues (purple and green lines in Figure 5c). However, copolymers **3** and **4** accumulated in the tumor tissues and exhibited contrast ratios as high as 1.5 after one day (red and blue lines in Figure 5c). In ex vivo experiments, fluorescence is obviously stronger in the tumor sites than in the kidneys, heart, and lungs (Figure 6), although uptake of copolymers **3** and **4** was found in the

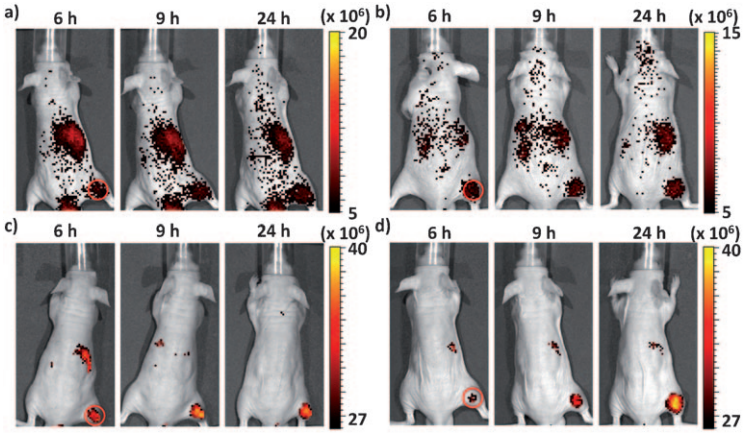

Figure 4. NIRF images (photons per second) of tumor-bearing mice after injection (after 6, 9, and 24 h) of 100 μL of ICG-containing self-assembled copolymers a) **1**, b) **2**, c) **3**, and d) **4** (5.0 mg mL^{-1}). Color code: low intensity black, high intensity yellow, and tumor site red circle. Thresholds were appropriately established: 5.0×10^6 (copolymers **1** and **2**) and 2.7×10^7 (copolymers **3** and **4**).

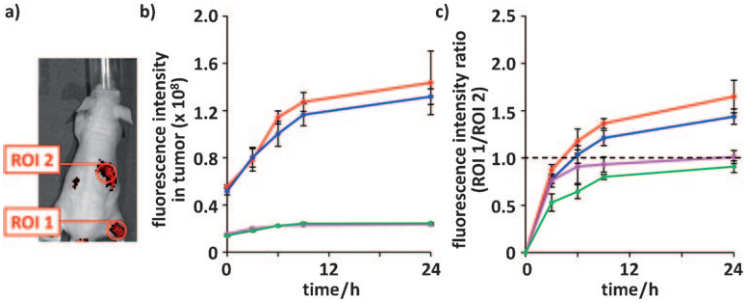

Figure 5. a) The regions of interest (ROIs), labeled by red circles of the same size, were studied in all imaging experiments displayed in Figure 4. ROI 1: tumor site and ROI 2: liver and kidney. b) Fluorescence intensity in a tumor site and c) fluorescence intensity ratios (ROI 1/ROI 2). Color code: Copolymer **1** green, copolymer **2** purple, copolymer **3** red, and copolymer **4** blue. The data are given as mean value ± standard deviation ($n=3$ per group).

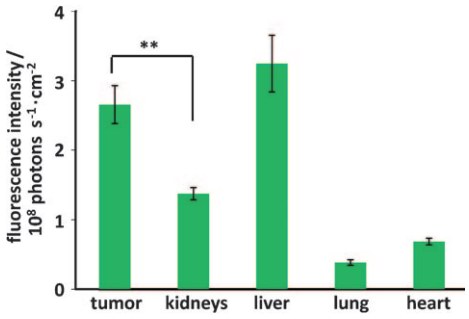

Figure 6. ROI analysis of the ex vivo NIRF imaging experiments (photons s^{-1} cm^{-2}) of dissected major organs of the tumor-bearing mice four days after intravenous injection of copolymer **3** (dose: 100 μL, 5 mg mL^{-1}). The data are given as mean value ± standard deviation ($n=3$). **: $p<0.01$.

liver.[21] The elongation of the side chains of copolymer **2** improved the fluorescence intensity of the nanoparticles (by 1.4–1.8 times), whereas the tumor selectivity decreased in in vivo imaging (see Figure S8 in the Supporting Information). This indicates that the tumor-targeting folate moieties prefer to hide inside the more hydrophobic environment because of the poor hydrophilicity of folic acid relative to that of the RGD peptides and GA moieties.[22] Considering the cac values of copolymers **1**–**4** shown in Table 1, it is likely that the cyclic RGD peptides and GA moieties localize on the surface of the hydrophilic PEG shells without hampering the formation of stable self-assemblies. Moreover, cyclic RGD peptides and GA moieties work effectively as active targeting agents, that is, the assemblies accumulate efficiently in the tumor tissues. Although it is difficult to explain the differences in the recognition processes of the targeting moieties in the tumor tissues,[23] these results clearly show that self-assembled brush-like copolymers with cyclic RGD peptides and GA moieties as targeting agents are better high-contrast optical imaging probes than the studied probes with and without folate moieties.

In summary, we have developed assemblies consisting of amphiphilic brush-like copolymers prepared through ROMP and grafting of PEG brushes. The assemblies with a partially cross-linked interface are sufficiently stable in aqueous media to accumulate in tumor tissues because of their EPR effect. Conjugation with cyclic RGD peptides and glucosamine molecules further enhanced their selectivity of tumors because these targeting agents, localized on the surface of the self-assemblies, effectively come in contact with tumor-specific ligands on tumor tissues. The present ROMP-based amphiphilic copolymers, used as imaging probes, accumulate rapidly and efficiently in targeted tumor tissues. The results might offer great potential, ideally not only for noninvasive and effective optical imaging, but also for biomedical applications, that is, for drug-releasing molecular medicines.

Experimental Section

Materials: Detailed information about the materials, preparation of copolymers **1**–**4**, characterization of their self-assemblies, and optical imaging experiments are provided in the Supporting Information.

Received: February 9, 2011
Revised: April 6, 2011
Published online: June 7, 2011

Keywords: fluorescence · imaging agents · interfaces · metathesis · polymers

[1] a) R. Weissleder, U. Mahmood, *Radiology* **2001**, *219*, 316; b) H. R. Herschman, *Science* **2003**, *302*, 605; c) C. Kim, C. Favazza, L. V. Wang, *Chem. Rev.* **2010**, *110*, 2756; d) H. Kobayashi, M. Ogawa, R. Alford, P. L. Choyke, Y. Urano, *Chem. Rev.* **2010**, *110*, 2620.

[2] For recent examples, see: a) A. Makino, S. Kizaka-Kondoh, R. Yamahara, I. Hara, T. Kanzaki, E. Ozeki, M. Hiraoka, S. Kimura, *Biomaterials* **2009**, *30*, 5156; b) I. Steppan, D. Reimer, U. Sevelda, H. Uimer, C. Marth, A. G. Zeimet, *Chemotherapy* **2009**, *55*, 391; c) T. A. ElBayoumi, V. P. Torchilin, *Clin Cancer Res.* **2009**, *15*, 1973; d) D. Mirchandani, H. Hochster, A. Hamilton, L. Liebes, H. Yee, J. P. Curtin, S. Lee, J. Sorich, C. Dellenbaugh, F. M. Muggia, *Clin. Cancer Res.* **2005**, *11*, 5912; e) A. S. A. Lila, Y. Doi, K. Nakamura, T. Ishida, H. Kiwada, *J. Controlled Release* **2010**, *142*, 167; f) Y. Anraku, A. Kishimura, M. Oba, Y. Yamasaki, K. Kataoka, *J. Am. Chem. Soc.* **2010**, *132*, 1631.

[3] a) D. E. Discher, A. Eisenberg, *Science* **2002**, *297*, 967; b) K. Hoste, K. D. Winne, E. Schacht, *Int. J. Pharm.* **2004**, *277*, 119; c) K. Osada, K. Kataoka, *Adv. Polym. Sci.* **2006**, *202*, 113; d) M. J. Vicent, R. Duncan, *Trends Biotechnol.* **2006**, *24*, 39; e) V. P. Torchilin, *Pharm. Res.* **2007**, *24*, 1; f) V. P. Torchilin, *AAPS J.* **2007**, *9*, E128.

[4] a) Y. Matsumura, H. Maeda, *Cancer Res.* **1986**, *46*, 6387; b) A. K. Iyer, G. Khaled, J. Fang, H. Maeda, *Drug Discovery Today* **2006**, *11*, 812.

[5] a) W. West, S. Pearce, *J. Phys. Chem.* **1965**, *69*, 1894; b) A.-K. Kirchherr, A. Briel, K. Mäder, *Mol. Pharm.* **2009**, *6*, 480, and references therein. Hydrophobic dyes are used as model payload to estimate the effectiveness of drug release because the fluorescence intensities of the dyes located inside/outside the self-assemblies are different in aqueous solution. See: c) E. R. Gillies, T. B. Jonsson, J. M. Fréchet, *J. Am. Chem. Soc.* **2004**, *126*, 11936; d) A. Klaikherd, C. Nagamani, S. Thayumanavan, *J. Am. Chem. Soc.* **2009**, *131*, 4830.

[6] For recent examples, see: a) H.-i. Lee, J. Pietrasik, S. S. Sheiko, K. Matyjaszewski, *Prog. Polym. Sci.* **2010**, *35*, 24, and references therein; b) D. Zehm, A. Laschewsky, M. Gradzielski, S. Prévost, H. Liang, J. P. Rabe, R. Schweins, J. Gummel, *Langmuir* **2010**, *26*, 3145; c) K. Ishizu, Y. Furuta, S. Nojima, S. Uchida, *J. Appl. Polym. Sci.* **2010**, *116*, 2298; d) Y.-Y. Yuan, Q. Du, Y.-C. Wang, J. Wang, *Macromolecules* **2010**, *43*, 1739; e) J.-Z. Du, L.-Y. Tang, W.-J. Song, Y. Shi, J. Wang, *Biomacromolecules* **2009**, *10*, 2169; f) P. Xu, S.-Y. Li, Q. Li, E. A. Van Kirk, J. Ren, W. J. Murdoch, Z. Zhang, M. Radosz, Y. Shen, *Angew. Chem.* **2008**, *120*, 1280; *Angew. Chem. Int. Ed.* **2008**, *47*, 1260.

[7] a) T. M. Trnka, R. H. Grubbs, *Acc. Chem. Res.* **2001**, *34*, 18; b) T.-L. Choi, R. H. Grubbs, *Angew. Chem.* **2003**, *115*, 1785; *Angew. Chem. Int. Ed.* **2003**, *42*, 1743.

[8] For recent examples, see: a) D. Smith, E. B. Pentzer, S. T. Nguyen, *Polym. Rev.* **2007**, *47*, 419; b) D. D. Smith, S. H. Clark, P. A. Bertin, B. L. Mirkin, S. T. Nguyen, *J. Mater. Chem.* **2009**, *19*, 2159; c) E. M. Kolonko, J. K. Pontrello, S. L. Mangold, L. L. Kiessling, *J. Am. Chem. Soc.* **2009**, *131*, 7327; d) J. B. Matson, R. H. Grubbs, *J. Am. Chem. Soc.* **2008**, *130*, 6731.

[9] a) K. Miki, Y. Kuramochi, K. Oride, S. Inoue, H. Harada, M. Hiraoka, K. Ohe, *Bioconjugate Chem.* **2009**, *20*, 511; b) K. Miki, K. Oride, S. Inoue, Y. Kuramochi, R. R. Nayak, H. Matsuoka, H. Harada, M. Hiraoka, K. Ohe, *Biomaterials* **2010**, *31*, 934.

[10] For recent examples, see: a) Z. Li, J. Ma, C. Cheng, K. Zhang, K. L. Wooley, *Macromolecules* **2010**, *43*, 1182; b) Y. Xia, B. D. Olsen, J. A. Kornfield, R. H. Grubbs, *J. Am. Chem. Soc.* **2009**, *131*, 18525.

[11] H. C. Kolb, M. G. Finn, K. B. Sharpless, *Angew. Chem.* **2001**, *113*, 2056 – 2075; *Angew. Chem. Int. Ed.* **2001**, *40*, 2004 – 2021.

[12] a) H. C. Kolb, M. S. VanNieuwenhze, K. B. Sharpless, *Chem. Rev.* **1994**, *94*, 2483 – 2547; b) P. Dupau, R. Epple, A. A. Thomas, V. V. Fokin, K. B. Sharpless, *Adv. Synth. Catal.* **2002**, *344*, 421 – 433.

[13] The ratio of hydrophobic/hydrophilic segments was optimized using copolymerization with different ratios of the monomers. The number of dye segments was also optimized using block or random copolymerization (see Table S5 and Figure S4 in the Supporting Information).

[14] Because the amount of the targeting agents used for the conjugation step was twice that of the ICG derivative, we suppose that the targeting agents and ICG moieties were introduced approximately in a 2:1 ratio.

[15] $\lambda_{max} = 790$ nm, $\varepsilon = 2.9 \times 10^4$ L mol^{-1} cm^{-1} (1.0×10^{-5} M in $CHCl_3$). This dye is soluble in polar organic solvents, but insoluble in aqueous solution.

[16] Because the brush-like copolymer **2′**, which is ten times larger than copolymer **2** at the same monomer ratio, formed nanoparticles with a similar diameter ($D_{DLS} = 198$ nm) in aqueous solution, we suppose that the main chains of the brush-like copolymers **1**–**4** and **2′** are bent and create a partially cross-linked interface.

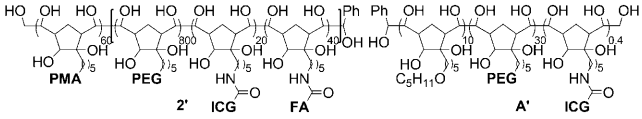

[17] The mean diameters of assemblies did not change for one week in phosphate-buffered saline at pH 7.4 (D_{DLS} ca. 200 nm).

[18] The human cervical epithelial adenocarcinoma cell line (HeLa) was subcutaneously inoculated in the right hind leg of a six-week-old nude mice. For more details of the imaging experiments, see the Supporting Information.

[19] For half-life times of copolymers **1**–**4** in blood vessels, see the Supporting Information.

[20] Tumor imaging experiments (Figure S6 in the Supporting Information) show that the brush-like copolymer **1** is more tumor-selective than copolymer **A′** without PMA side chains (cac = 4.4×10^{-4} g L^{-1}).

[21] For the ex vivo experiment of copolymer **4**, see Figure S7 in the Supporting Information. Although the fluorescence intensities in tumor tissues were stronger than those in normal tissues observed by optical in vivo imaging, the fluorescence intensities in the harvested liver were 1.2–1.3 times stronger than those in the harvested tumor tissues. This observation might be caused by underestimation of the fluorescence from normal tissues in the ventral cavity. Although further improvement is necessary for diagnostic purposes, the present high-contrast optical imaging technique using polymeric self-assemblies is broadly applicable to facile detection of subcutaneous tumor tissues by endoscopy or at surgery.

[22] Folic acid is scarcely soluble in aqueous solution (< 1 mg mL^{-1}), whereas glucosamine molecuels and cyclic RGD peptides are much better water-soluble (> 10 mg mL^{-1}).

[23] For folate-receptor targeting, see: P. S. Low, W. A. Henne, D. D. Doorneweerd, *Acc. Chem. Res.* **2008**, *41*, 120. For $\alpha_v\beta_3$ integrin-binding RGD peptides, see: W. Arap, R. Pasqualini, E. Ruoslahti, *Science* **1998**, *279*, 377. For glucose-transporting systems that recognize glucosamine, see: Z. Cheng, J. Levi, Z. Xiong, O. Gheysens, S. Keren, X. Chen, S. S. Gambhir, *Bioconjugate Chem.* **2006**, *17*, 662, and references therein. For binding studies of the targeting agents, see the Supporting Information.

